Electric field induced modulation of transverse resistivity anomalies in ultrathin $SrRuO_3$ epitaxial films

Daisuke Kan,[1,*] Kento Kobayashi,[1] and Yuichi Shimakawa[1,2]
[1]*Institute for Chemical Research, Kyoto University, Uji, Kyoto 611-0011, Japan*
[2]*Integrated Research Consortium on Chemical Sciences, Uji, Kyoto 611-0011, Japan*

(Received 9 January 2020; revised manuscript received 1 March 2020; accepted 19 March 2020; published 6 April 2020)

We show that transverse resistivity anomalies in $SrRuO_3$ epitaxial thin films, which have been claimed to be a manifestation of the topological Hall effect, can be modulated by applying gate voltages (V_G). The electric field induced effects on the anomalies are found to be the same as those of the saturated anomalous Hall resistivity (ρ_{AHE}), revealing that the anomalies arise as a result of the coexistence of the intrinsic and extrinsic ρ_{AHE}. Furthermore, the V_G-induced effects on the anomalies are dominated by the V_G-induced changes in the intrinsic ρ_{AHE} while the extrinsic ρ_{AHE} remains unchanged under the V_G applications. Our results reveal that electric field induced modulations in the anomalous Hall effect depend on its mechanism.

DOI: 10.1103/PhysRevB.101.144405

I. INTRODUCTION

For magnetic materials in which conduction electrons are closely coupled with magnetization, a Berry curvature originated fictitious magnetic field plays key roles in their transport properties as manifested in the anomalous Hall effect (AHE) in ferromagnets and antiferromagnets and in the topological Hall effect [1–9]. Given that Berry curvatures are often correlated to (topologically) nontrivial electronic structures and magnetic spin textures, electric field tunings of the Fermi level (E_F) position and motions of conduction electrons (or orbitals) are expected to modulate and even enhance such Hall effects, enabling exploration of intriguing magnetotransport phenomena.

Perovskite strontium ruthenate $SrRuO_3$ (SRO) is known to be an itinerant ferromagnet whose AHE is dominantly contributed by the Berry curvature arising from multiple band crossings around the E_F [10–12]. The magnitude and sign of the intrinsic anomalous Hall resistivity ρ_{AHE} change nonmonotonically with temperature, while the magnetization changes monotonically [11,13–16]. It has also been shown that gating SRO with positive and negative biases, respectively, increases and decreases ρ_{AHE}, allowing us to modulate both the magnitude and sign of ρ_{AHE} (or the anomalous Hall conductivity) [17–19]. These electric field induced effects are attributed to gate voltage (V_G) induced changes in an integral of the Berry curvature over the filled electronic states, which are proportional to AHE.

Recently, ultrathin films of SRO were also reported to exhibit anomalies in transverse (Hall) resistivity ρ_{xy} that were seen as hump structures (referred to as hump resistivity, ρ_{hump}) in the magnetic-field dependence of ρ_{xy} [20–27]. The anomalies cannot be explained by the conventional framework of AHE and are often attributed to the emergence of the topological Hall effect (THE) due to formations of topologically nontrivial magnetic textures such as skyrmions. However, such topological magnetic textures have not been experimentally observed for SRO films and the origin of the anomalies (or ρ_{hump}) has been under debate. In fact, alternatives to the topological interpretation of the anomalies have been proposed [23,24,28,29]. As shown in Fig. 1, inhomogeneity in coercive field (H_c) and ρ_{AHE} (coexistence of positive and negative ρ_{AHE}) has been shown to explain the emergence of hump structures in the ρ_{xy}-H curves (or ρ_{hump}). Given the V_G-induced modulations on ρ_{AHE} in SRO, investigating V_G-induced effects on ρ_{hump} would provide insight on its origin. If ρ_{hump} arises from formation of skyrmions, its origin totally differs from AHE, and responses of ρ_{hump} and ρ_{AHE} to gate biases (V_G) should be distinct. It is also worth mentioning that behavior of ρ_{hump} under V_G applications would provide insight on the alternative scenarios for ρ_{hump}, as discussed in the caption to Fig. 1. If the magnitude of ρ_{AHE} is spatially inhomogeneous but the origin of ρ_{AHE} is common (for example, the intrinsic mechanism), V_G-induced changes in ρ_{AHE} should be seen independent of its magnitude and sign. In this case [Fig. 1(b)], V_G-induced changes in ρ_{AHE} are compensated in the magnetic-field regions where ρ_{hump} is seen, and the V_G-induced effects on ρ_{hump} are expected to be less pronounced than those for the saturated ρ_{AHE}. On the other hand, if inhomogeneous ρ_{AHE} is a result of coexistence of ρ_{AHE} whose mechanisms are different (for example, intrinsic and extrinsic mechanisms), responses of ρ_{AHE} against V_G should depend on its mechanism. Given that extrinsic ρ_{AHE} are expected to be less influenced by V_G-induced modulations in electron fillings in the conduction bands, V_G-induced effects on ρ_{hump} are dominated only by V_G-induced changes in intrinsic ρ_{AHE} [Fig. 1(c)].

In this study we investigated electric field induced effects on transverse resistivity anomalies (hump resistivity, ρ_{hump})

*dkan@scl.kyoto-u.ac.jp

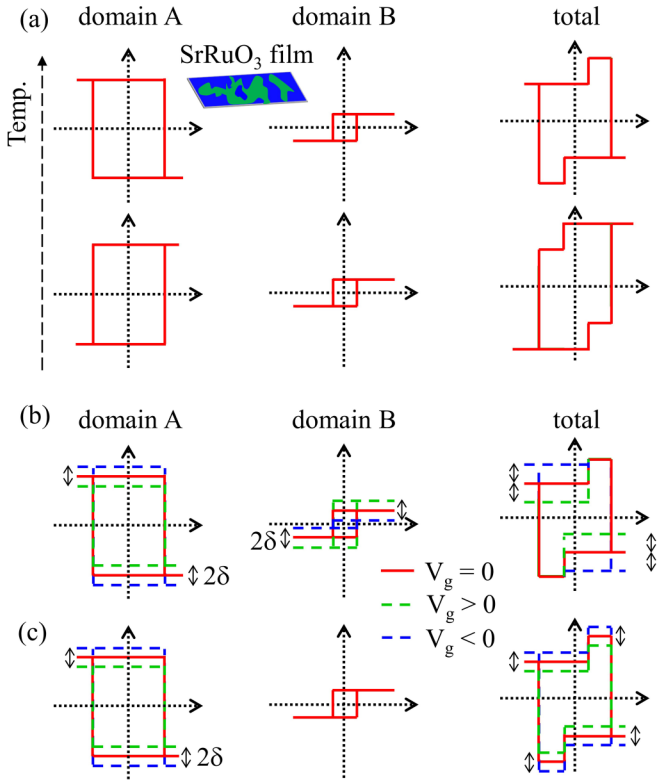

FIG. 1. (a) Schematics of the alternative model for transverse resistivity anomalies (hump resistivity, $\rho_{\rm hump}$) in $SrRuO_3$. Inhomogeneity in the coercive field H_c and the anomalous Hall resistivity $\rho_{\rm AHE}$ are taken into consideration. (b), (c) Possible models for gate voltage (V_G) induced effects on the transverse resistivity anomalies in $SrRuO_3$. In (b) the anomalous Hall resistivities $\rho_{\rm AHE}$ in both domains A and B are electrically modulated. As a consequence of compensations in V_G-induced changes in $\rho_{\rm AHE}$, $\rho_{\rm hump}$ is expected to remain unchanged under V_G applications. On the other hand, in (c) the $\rho_{\rm AHE}$ only in domain A is electrically modulated while the $\rho_{\rm AHE}$ in domain B remains unchanged under V_G applications. In this case, the V_G-induced changes in $\rho_{\rm hump}$ in the SRO film follow the V_G-induced changes in the saturated $\rho_{\rm AHE}$ in the domain A.

in SRO thin films. We found that applying gate voltages into SRO modulates $\rho_{\rm hump}$. Based on electric field induced changes in $\rho_{\rm hump}$, its origin is discussed.

II. EXPERIMENTAL DETAILS

To investigate electric field induced effects on transverse resistivity ρ_{xy} in SRO, we fabricated field-effect transistor structures with a channel layer of SRO. The channel layer (3 nm thick) was grown on (110) $NdGaO_3$ substrates by pulsed laser deposition. The epitaxial growth of the SRO layer on the substrates was confirmed by x-ray-diffraction characterizations and the layer's thickness was determined from x-ray reflectivity measurements. Details of the film growth were given in our previous papers [23,30]. To fabricate field-effect transistor structures, the SRO layer was patterned into a 30-μm-wide Hall bar by conventional photolithography and Ar ion milling. A 50-nm-thick HfO_2 layer as a gate insulator was subsequently deposited by atomic layer deposition. We confirmed that the SRO channel layer in the fabricated

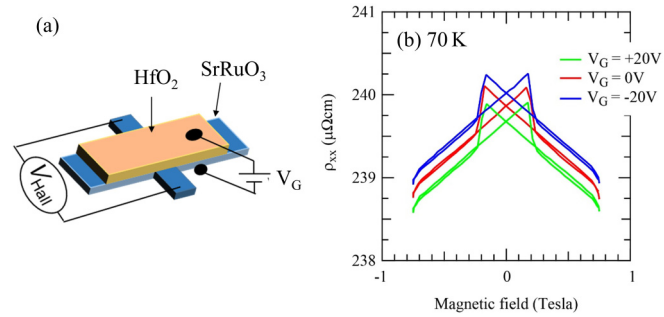

FIG. 2. (a) Device configuration. (b) Magnetic-field dependence of the electrical resistivity ρ_{xx} of the SRO film under $V_G = +20$, 0, and -20 V at 70 K.

transistor structure exhibits metallic conduction down to low temperatures and undergoes a ferromagnetic transition around 130 K.

III. RESULTS AND DISCUSSION

We begin with the V_G-induced effects on the longitudinal resistivity ρ_{xx} of the SRO channel. Figure 2 shows the device configuration and magnetic-field dependence of ρ_{xx} under $V_G = +20$, 0, and -20 V at 70 K. We confirmed that when the gate voltages of $+20$ and -20 V were applied, the leak current through the gate insulator layer was less than 100 pA. Under $V_G = 0$ V, the channel exhibits negative magnetoresistance whose magnitude is about 0.3% at 5000 Oe. In our device configuration, applying positive and negative V_G are, respectively, expected to accumulate and deplete about 10^{18} cm^{-3} electron carriers into the channels. The expected carrier density was calculated by assuming that the HfO_2 gate insulating layer has a dielectric constant of 20 and is under $V_G = 20$ V. In fact, applying V_G of $+20$ and -20 V, respectively, decreases and increases ρ_{xx}, while the magnitude of the magnetoresistance remains unchanged by the V_G applications. Note that essentially the same V_G-induced changes in ρ_{xx} at 70 K are seen at all measuring temperatures. These behaviors of ρ_{xx} under V_G are in close agreements with previous reports on V_G-induced effects in SRO films [17,19]. The V_G-induced changes in ρ_{xx} therefore indicate that by applied V_G the channels are electrostatically accumulated and depleted, and consequently the Berry curvature integrated over the filled electronic states is changed, leading to the modulations in ρ_{xy} in the SRO channel.

We then turn our attention to the transverse resistivity ρ_{xy} in the SRO channel layer under V_G. Figure 3 shows magnetic-field dependence of ρ_{xy} under $V_G = +20$, 0, and -20 V. By taking the difference between the data measured at positive and negative magnetic fields and normalizing the readings, we corrected asymmetric components in measured Hall resistivity that resulted from misalignments of samples. To obtain ρ_{xy} that are associated with the magnetization, the ordinary part of the Hall resistivity was determined by linearly fitting the data in the higher magnetic-field region and was subtracted from the antisymmetrized Hall resistivity. We first pay attention to ρ_{xy}-H curves under $V_G = 0$ V. With decreasing temperature, the magnitude of the saturated $\rho_{\rm AHE}$

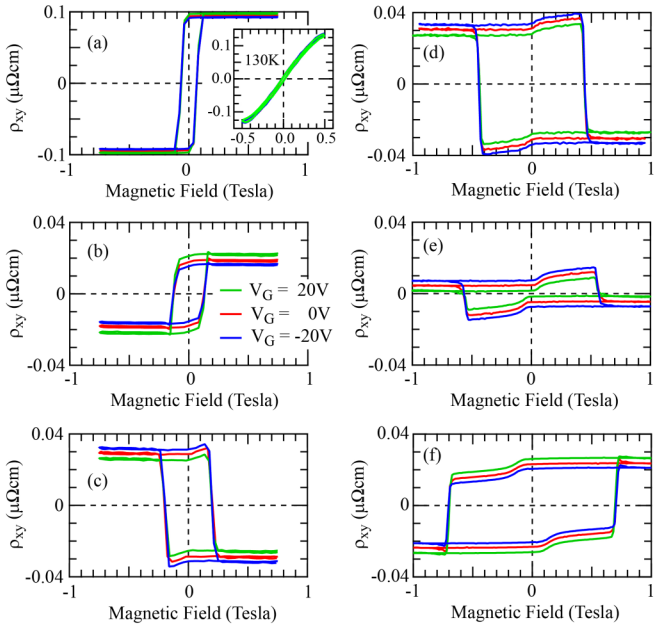

FIG. 3. Magnetic-field dependence of the transverse resistivity ρ_{xy} of the SRO channel layer under $V_G = +20$, 0, and -20 V. The ρ_{xy}-H curves were taken at (a) 90 K, (b) 80 K, (c) 70 K, (d) 40 K, (e) 30 K, and (f) 20 K. The inset in (a) shows the magnetic-field dependence of ρ_{xy} under $V_G = +20$, 0, and -20 V at 130 K.

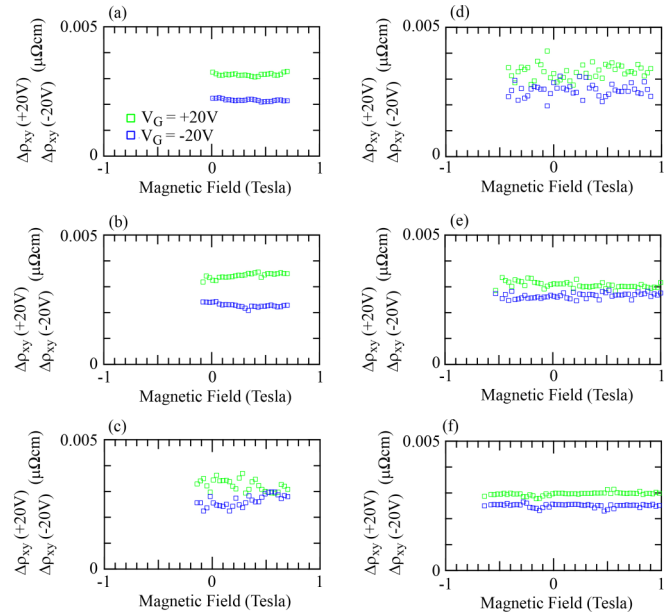

FIG. 4. V_G-induced changes in ρ_{xy}, $\Delta\rho_{xy}(V_G)$ of the SRO channel layer as a function of the magnetic field at (a) 90 K, (b) 80 K, (c) 70 K, (d) 40 K, (e) 30 K, and (f) 20 K.

in the SRO layer nonmonotonically changes and its sign also reverses. These observations are in close agreements with previous reports on magnetotransport characterizations of SRO films [11,13,15,16]. Furthermore, hump structures (hump resistivity, ρ_{hump}) are seen in the ρ_{xy}-H curves at temperatures below 80 K and the magnetic-field regions in which ρ_{hump} is seen are expanded at lower temperatures. The ρ_{hump} is positive independent of the measuring temperatures. The whole shape of the ρ_{xy}-H curves can be understood by taking into account inhomogeneity of both AHE and H_c. As shown in Fig. 1(a), we simply consider that the film consists of two magnetic domains (domains A and B) that have distinct ρ_{AHE} and H_c. The ρ_{AHE} of the domain A nonmonotonically changes and its sign reverses with changes in the temperature, which can be attributed to the intrinsic ρ_{AHE} in the SRO films. On the other hand, the ρ_{AHE} of the domain B is relatively small and is positive independent of temperature. In addition, the H_c in the domain A is much larger than that in the domain B. This simple model can reproduce the temperature-dependent changes in the ρ_{xy}-H curves (Fig. 2). We note that the magnetic-field region where the ρ_{hump} is seen is determined by the difference in H_c between the domains A and B.

We now turn our attention to V_G-induced effects on ρ_{hump}. Regardless of measuring temperatures below the ferromagnetic transition temperature (Tc), applying V_G is found to modulate ρ_{xy} including ρ_{hump}. Note that at temperatures above Tc, no V_G-induced changes in ρ_{xy} are seen [the inset of Fig. 3(a)]. At 80 K where ρ_{AHE} is positive, the applications of $V_G = +20$ and -20 V, respectively, induce an increase and decrease in ρ_{xy}. While the ρ_{AHE} is negative at 70 K, essentially the same V_G-induced changes in the ρ_{xy} are also seen at this temperature. Although the observed V_G-induced changes in the ρ_{xy} do not follow what is expected from the monotonic change of the magnetization with the temperature [10,14], the V_G-induced increase and decrease in ρ_{xy} are consistently seen at all measuring temperatures (Fig. 3), and are in close agreement with previous reports on electric field induced effects on ρ_{AHE} in SRO [17–19].

Importantly, the V_G-induced changes in ρ_{hump} follow the same trend as that of the saturated ρ_{AHE}. Regardless of the sign of ρ_{AHE}, increase and decrease in ρ_{hump} are induced by the applications of positive and negative V_G, respectively. To quantitatively evaluate the V_G-induced changes in ρ_{hump}, we calculated $\Delta\rho_{xy}(V_G) = |\rho_{xy}(V_G) - \rho_{xy}(0\,\mathrm{V})|$ from the ρ_{xy} measured by sweeping down the magnetic field. Figure 4 shows the magnetic-field dependence of $\Delta\rho_{xy}(V_G)$ ($V_G = +20$ and -20 V). For both $V_G = +20$ and -20 V cases, $\Delta\rho_{xy}(V_G)$ is almost constant against the magnetic field. No obvious changes in $\Delta\rho_{xy}(V_G)$ are seen in the magnetic fields at which ρ_{hump} appear. This indicates that the origins of ρ_{hump} and ρ_{AHE} are the same, implying that topologically nontrivial magnetic structures are unlikely to form in the magnetic fields at which ρ_{hump} is seen. Our observations can be understood by the model that ρ_{hump} originate from the inhomogeneity of ρ_{AHE} and H_c within the film (Fig. 1). Furthermore, the observations that the V_G-induced changes in the ρ_{hump} and the saturated ρ_{AHE} are the same magnitudes indicate that the ρ_{xy} in SRO consists of ρ_{AHE} originating from distinct mechanisms—i.e., intrinsic and extrinsic mechanisms—and that the V_G-induced changes in the ρ_{hump} are dominated by those in the intrinsic ρ_{AHE} [Fig. 1(c)]. Only the intrinsic ρ_{AHE} that nonmonotonically changes with temperature contributes to the V_G-induced changes in ρ_{xy} while the extrinsic ρ_{AHE} that is positive independent of temperature remains unchanged under V_G applications. This can consistently explain our observed V_G-induced effect on ρ_{xy} in the SRO film.

Finally, it should be pointed out that in SRO films grown by pulsed laser deposition, point defects are easily introduced through formations of Ru vacancies and local island growth resulting from mixed termination layers of substrates [31–33]. Such defects would not only reduce H_c in local regions but also provide additional transverse scatterings of conduction carriers, and the influence of such defects probably is enhanced when film thickness is reduced and comparable to spatial extents of defects' potentials, leading to the formation of the domain B in Fig. 1(a). Therefore, the transverse resistivity in the ultrathin SRO films is additionally contributed by the extrinsic ρ_{AHE}. The resultant coexistence of the intrinsic and extrinsic ρ_{AHE}, namely the coexistence of the domains A and B, leads to the emergence of the transverse resistivity anomalies (the hump resistivity). The mechanism dependence of the electric field induced effects in ρ_{AHE} is the reason why the V_G-induced effects on the hump resistivity are the same as those of ρ_{AHE}.

IV. SUMMARY

We show that the transverse resistivity anomalies (the hump resistivity, ρ_{hump}) in the SRO channel layer in the field-effect transistor structure are modulated by applied gate voltages V_G. The applications of positive and negative V_G, respectively, increase and decrease ρ_{hump}. We also found that the V_G-induced changes in ρ_{hump} are essentially the same as those of the saturated ρ_{AHE}. These observations indicate that the transverse resistivity anomalies emerge as a result of the coexistence of the anomalous Hall resistivity with distinct mechanisms, i.e., intrinsic and extrinsic anomalous Hall resistivity. Topological interpretation such as formations of topologically nontrivial magnetic structures is not necessary. Furthermore, the V_G-induced changes in ρ_{hump} are dominated by the intrinsic ρ_{AHE} while the extrinsic ρ_{AHE} remains unchanged under the V_G applications. Our results reveal that electric field induced changes in the anomalous Hall effect depend on its mechanism.

ACKNOWLEDGMENTS

This work was partially supported by a grant for the Integrated Research Consortium on Chemical Sciences, by Grants-in-Aid for Scientific Research (Grants No. JP16H02266, No. JP17H05217, and No. JP17H04813), by a JSPS Core-to-Core program (A), and by a grant for the Joint Project of Chemical Synthesis Core Research Institutions from the Ministry of Education, Culture, Sports, Science, and Technology (MEXT) of Japan.

[1] N. Nagaosa, J. Sinova, S. Onoda, A. H. MacDonald, and N. P. Ong, Rev. Mod. Phys. **82**, 1539 (2010).
[2] T. Jungwirth, Q. Niu, and A. H. MacDonald, Phys. Rev. Lett. **88**, 207208 (2002).
[3] Y. Yao, L. Kleinman, A. H. MacDonald, J. Sinova, T. Jungwirth, D.-S. Wang, E. Wang, and Q. Niu, Phys. Rev. Lett. **92**, 037204 (2004).
[4] Y. Taguchi, Y. Oohara, H. Yoshizawa, N. Nagaosa, and Y. Tokura, Science **291**, 2573 (2001).
[5] S. Nakatsuji, N. Kiyohara, and T. Higo, Nature (London) **527**, 212 (2015).
[6] T. Suzuki, R. Chisnell, A. Devarakonda, Y. T. Liu, W. Feng, D. Xiao, J. W. Lynn, and J. G. Checkelsky, Nat. Phys. **12**, 1119 (2016).
[7] A. Neubauer, C. Pfleiderer, B. Binz, A. Rosch, R. Ritz, P. G. Niklowitz, and P. Böni, Phys. Rev. Lett. **102**, 186602 (2009).
[8] P. Bruno, V. K. Dugaev, and M. Taillefumier, Phys. Rev. Lett. **93**, 096806 (2004).
[9] N. Nagaosa and Y. Tokura, Nat. Nanotechnol. **8**, 899 (2013).
[10] G. Koster, L. Klein, W. Siemons, G. Rijnders, J. S. Dodge, C.-B. Eom, D. H. A. Blank, and M. R. Beasley, Rev. Mod. Phys. **84**, 253 (2012).
[11] Z. Fang, N. Nagaosa, K. S. Takahashi, A. Asamitsu, R. Mathieu, T. Ogasawara, H. Yamada, M. Kawasaki, Y. Tokura, and K. Terakura, Science **302**, 92 (2003).
[12] S. Itoh, Y. Endoh, T. Yokoo, S. Ibuka, J.-G. Park, Y. Kaneko, K. S. Takahashi, Y. Tokura, and N. Nagaosa, Nat. Commun. **7**, 11788 (2016).
[13] M. Izumi, K. Nakazawa, Y. Bando, Y. Yoneda, and H. Terauchi, J. Phys. Soc. Jpn. **66**, 3893 (1997).
[14] G. Cao, S. McCall, M. Shepard, J. E. Crow, and R. P. Guertin, Phys. Rev. B **56**, 321 (1997).
[15] Y. Kats, I. Genish, L. Klein, J. W. Reiner, and M. R. Beasley, Phys. Rev. B **70**, 180407(R) (2004).
[16] N. Haham, Y. Shperber, M. Schultz, N. Naftalis, E. Shimshoni, J. W. Reiner, and L. Klein, Phys. Rev. B **84**, 174439 (2011).
[17] H. Mizuno, K. T. Yamada, D. Kan, T. Moriyama, Y. Shimakawa, and T. Ono, Phys. Rev. B **96**, 214422 (2017).
[18] Y. Ohuchi, J. Matsuno, N. Ogawa, Y. Kozuka, M. Uchida, Y. Tokura, and M. Kawasaki, Nat. Commun. **9**, 213 (2018).
[19] S. Shimizu, K. S. Takahashi, M. Kubota, M. Kawasaki, Y. Tokura, and Y. Iwasa, Appl. Phys. Lett. **105**, 163509 (2014).
[20] J. Matsuno, N. Ogawa, K. Yasuda, F. Kagawa, W. Koshibae, N. Nagaosa, Y. Tokura, and M. Kawasaki, Sci. Adv. **2**, e1600304 (2016).
[21] L. Wang, Q. Feng, Y. Kim, R. Kim, K. H. Lee, S. D. Pollard, Y. J. Shin, H. Zhou, W. Peng, D. Lee, W. Meng, H. Yang, J. H. Han, M. Kim, Q. Lu, and T. W. Noh, Nat. Mater. **17**, 1087 (2018).
[22] Q. Qin, L. Liu, W. Lin, X. Shu, Q. Xie, Z. Lim, C. Li, S. He, G. M. Chow, and J. Chen, Adv. Mater. **31**, 1807008 (2018).
[23] D. Kan, T. Moriyama, K. Kobayashi, and Y. Shimakawa, Phys. Rev. B **98**, 180408(R) (2018).
[24] D. Kan and Y. Shimakawa, Phys. Status Solidi B **255**, 1800175 (2018).
[25] B. Sohn, B. Kim, J. W. Choi, S. H. Chang, J. H. Han, and C. Kim, Curr. Appl. Phys. **20**, 186 (2020).
[26] G. Youdi, W. Yi-Wen, X. Kun, Z. Hongrui, W. Fei, L. Fan, S. Muhammad Shahrukh, C. Cui-Zu, S. Jirong, S. Cheng, F. Ji, Z. Xiaoyan, L. Wei, Z. Zhi-Dong, Z. Jing, and P. Feng, J. Phys. D: Appl. Phys. **52**, 404001 (2019).

[27] W. Wang, M. W. Daniels, Z. Liao, Y. Zhao, J. Wang, G. Koster, G. Rijnders, C.-Z. Chang, D. Xiao, and W. Wu, Nat. Mater. **18**, 1054 (2019).
[28] L. Wu and Y. Zhang, arXiv:1812.09847.
[29] A. Gerber, Phys. Rev. B **98**, 214440 (2018).
[30] D. Kan, M. Anada, Y. Wakabayashi, H. Tajiri, and Y. Shimakawa, J. Appl. Phys. **123**, 235303 (2018).
[31] B. Kuiper, J. L. Blok, H. J. W. Zandvliet, D. H. A. Blank, G. Rijnders, and G. Koster, MRS Commun. **1**, 17 (2011).
[32] R. Bachelet, F. Sánchez, J. Santiso, C. Munuera, C. Ocal, and J. Fontcuberta, Chem. Mater. **21**, 2494 (2009).
[33] W. Siemons, G. Koster, A. Vailionis, H. Yamamoto, D. H. A. Blank, and M. R. Beasley, Phys. Rev. B **76**, 075126 (2007).